THE AMERICAN MINERALOGIST, VOL. 53, SEPTEMBER–OCTOBER, 1968

CALCULATED POWDER PATTERNS: I. FIVE PLAGIOCLASES

I. Y. BORG AND D. K. SMITH, *Lawrence Radiation Laboratory University of California, Livermore, California.*

ABSTRACT

As an aid in indexing complex plagioclase X-ray powder patterns, integrated (I_{INT}) and peak (I_P) intensities are calculated for five plagioclases [low and high albite (An_0), oligoclase (An_{29}), bytownite (An_{80}) and anorthite (An_{100})]. Lorentz-polarization, absorption and multiplicity corrections appropriate to powder mounts are applied to temperature-corrected $|F|^2$ which are calculated from single-crystal structure analyses. Graphical expression of I_P as a function of 2θ results in plots which are very similar to the comparable experimental X-ray diffraction traces.

PREAMBLE

X-ray diffraction data are indispensable in modern studies of the plagioclase feldspars. Extensive studies relating lattice parameters to composition and conditions of crystallization have laid the basis for advanced studies on the relation of feldspars to other minerals. Many studies involve the use of x-ray powder patterns and require the reduction of complex patterns to yield the unit-cell dimensions. The assignment of Miller indices, *hkl*, to the observed diffraction maxima to obtain data for a least-squares refinement is a usual step in the data reduction process. The low symmetry of the plagioclases, their pseudo-symmetry (low obliquity), and rather large unit cells result in powder patterns of closely spaced and overlapped maxima. Because of rapid changes in cell constants with composition, as well as small changes in intensity related to composition, atomic distribution (disorder) and atomic coordinates, reliable and general guides to correct indexing, are precluded. For example, separating the approximately 120 reflections with intensities greater than 2 in the first 65°, 2θ range of anorthite is virtually impossible with only approximate cell dimensions and the spacings calculated from them. Intensity data are necessary to identify the reflections that contribute to each observed maximum. Such intensity data may be obtained from careful study of a series of powder patterns over the whole compositional and disorder range; however, some question usually remains as to the correct identity of some lines.

A better guide to relative *hkl* intensities is structure factors conventionally tabulated in descriptions of single-crystal structure analyses. For complex structures like the feldspars these tables are generally too numerous for publication, and are only available upon specific request to the investigators. Even when such tables are in hand, for the purpose of comparison with powder data, they must be interpreted in terms of the absorption, Lorentz-polarization, and multiplicity corrections applicable to powder samples. Therefore, in order to put the data from structure analyses in a more convenient form for use with powder patterns, sets of X-ray intensities have been calculated for five plagioclases.

Source of Data for Calculations

The five plagioclases for which powder patterns have been calculated include low and high albite, An_0 (Ribbe, Megaw, and Taylor, 1968); oligoclase, An_{29} (Colville and Ribbe, 1966); bytownite "body-centered anorthite," An_{80} (Fleet, Chandrasekhar, and Megaw, 1966); and anorthite, An_{100} (Kempster, Megaw, and Radoslovich, 1961). Results of calculations for transitional anorthite, An_{99} (Ribbe and Megaw, 1963) are not tabulated because of their similarity to those of anorthite; however, a calculated pattern is displayed for comparison. The chief difference in the two structures lies in the presence of sharp, very weak "*d*" reflections, and sharp, medium strong "*c*" reflections in anorthite. A resumé of pertinent parameters is given in Table 1. Minor K, Na, and Ca were generally ignored in the structural refinements and, as a consequence, the albites and anorthite were treated as pure $NaAlSi_3O_8$ and $CaAl_2Si_2O_8$, respectively, in results of calculations presented here. A random distribution was assumed on the Na/Ca sites for oligoclase and bytownite. All data were derived from three-dimensional structure analyses.

Calculations

The calculated intensities and spacings tabulated in Tables 2–7 were calculated from Smith's (1967, 1968) program for calculating powder diffraction patterns. Required input data include unit-cell dimensions, space group, atomic coordinates including site occupancy, temperature factors, and atomic scattering factors. If absorption corrections appropriate to the shape of the shape (in this case a cylinder or flat plate) are to be applied, linear absorption coefficients or density, atomic weights, and mass absorption coefficients are also needed. After a temperature-corrected $|F|^2$ is calculated, multiplicity, Lorentz-polarization corrections, and absorption factors are applied to give an integrated intensity for each *hkl* reflection permitted by the space group.

The decision to calculate structure factors rather than use published values of $|F_{obs}|$ or $|F_{calc}|$ is in consideration of the voluminous amount of input and attendant errors that are thereby eliminated. Agreement between $|F_{calc}|$ generated by the program and $|F_{calc}|$ published by the original researchers is a convenient check on the accuracy of the input used to generate the calculated powder intensities.

The calculated integrated intensity (I_{INT}) is directly proportional to the total energy per unit time for each diffraction event, and is independent of instrumental errors and

TABLE 1. DESCRIPTION OF PLAGIOCLASES

Variety Composition		Low Albite $Ab_{98.5}An_{0.5}$-$Or_{1.0}$	High Albite $Ab_{97.7}An_{0.7}$-$Or_{1.6}$	Oligoclase $Ab_{69}An_{29}$-Or_2	Bytownite $\sim Ab_{20}An_{80}$	Anorthite $\sim Ab_0An_{100}$
Source		Ramona, Calif.	Amelia, Va. (Inverted from low form)	Mitchell Co., N. C.	St. Louis Co., Minn.	Monte Somma, Italy
a (Å)		8.138	8.149	8.169	8.178	8.1768
b		12.789	12.880	12.851	12.870	12.8768
c		7.156	7.106	7.124	14.187	14.1690
α (deg)		94.33°	93.37°	93.63°	93.50°	93.17°
β		116.57°	116.30°	116.40°	115.90°	115.85°
γ		87.65°	90.28°	89.46°	90.63°	91.22°
Space group		$C\bar{1}$	$C\bar{1}$	$C\bar{1}$	$I\bar{1}$	$P\bar{1}$
Site occupancy (% Si)						
$T_1(0)$	(0000)	0[a]	72[a]	35	100	100
	(00i0)				100	100
	(0z00)	0	72	35	6	0
	(0zi0)				0	0
$T_1(m)$	(m000)	100	75	81	13	0
	(m0i0)				13	0
	(mz00)	100	75	81	100	100
	(mzi0)				100	100[b]
$T_2(0)$	(0000)	100	78	79	30	0
	(00i0)				13	0
	(0z00)	100	78	79	100	100
	(0zi0)				100	100
$T_2(m)$	(m000)	100	75	81	100	100
	(m0i0)				90	100[b]
	(mz00)	100	75	81	13	0
	(mzi0)				13	0
R		0.068	0.082	0.069	0.118	0.111
Reference		Ribbe *et al.* (1968) Ferguson *et al.* (1958)	Ribbe *et al.* (1968) Ferguson *et al.* (1958)	Colville & Ribbe (1966)	Fleet *et al.* (1966)	Kempster *et al.* (1962); Megaw *et al.* (1962); Cole *et al.* (1951)

[a] Ribbe, personal communication, 1968.

[b] These sites are reported to contain 10% Al (Megaw *et al.*, 1962, p. 1023), but because strain effects can limit the accuracy of apparent site occupancy to ±5%, for simplicity these sites aıe considered to be 100% Si in subsequent calculations (Fleet *et al.* (1966) p. 797).

other abberations. The peak intensity (I_P), on the other hand, is not so easily interpreted because it is sensitive to the real dispersion of the diffracted waves producing the maximum.

TABLE 2. CALCULATED POWDER DATA FOR LOW ALBITE (An_0)

2θ(INT)	2θ(P)	d	hkℓ	I_{INT}	I_P	2θ(INT)	2θ(P)	d	hkℓ	I_{INT}	I_P
13.86		6.387	001	7		49.97	49.98	1.825	$0\bar{4}3$	5	9
13.89	13.88	6.376	020	4	9	50.00		1.824	$0\bar{6}2$	7	
13.96		6.343	110	3		50.13	50.13	1.820	400	12	9
14.06		6.299	$\bar{1}10$	3		50.63	50.64	1.803	113	9	5
14.99	14.99	5.912	$\bar{1}\bar{1}1$	4	2	51.21	51.21	1.784	$\bar{2}04$	20	10
15.88	15.88	5.581	$\bar{1}11$	4	3	52.16	52.18	1.753	420	2	3
22.07	22.07	4.027	$\bar{2}01$	93	61	52.19		1.753	$\bar{2}\bar{2}4$	4	
23.08	23.08	3.854	$1\bar{1}1$	15	11	52.54	52.54	1.742	$\bar{4}\bar{4}2$	7	4
23.56	23.56	3.777	111	39	26	53.21		1.721	$2\bar{4}2$	3	
24.16	24.18	3.684	130	22	21	53.28		1.719	062	3	
24.26	24.32	3.668	$\bar{1}\bar{3}1$	16	34	53.32	53.32	1.718	$1\bar{3}3$	3	6
24.33		3.658	$\bar{1}30$	42		53.35		1.717	$\bar{4}\bar{4}1$	2	
25.41	25.41	3.505	$\bar{1}\bar{1}2$	15	10	53.35		1.717	$\bar{2}62$	4	
25.57	25.57	3.483	$\bar{2}\bar{2}1$	6	5	54.44	54.44	1.685	$\bar{2}24$	4	2
26.44	26.44	3.370	$\bar{1}12$	16	10	55.09	55.09	1.667	242	4	3
27.76	27.76	3.214	$\bar{2}02$	72	58	57.84	57.84	1.594	080	2	2
27.94		3.194	002	100		58.18	58.20	1.586	$\bar{3}53$	4	3
27.99	27.96	3.188	040	66	100	58.20		1.585	$\bar{4}\bar{2}4$	3	
28.13		3.172	220	37		58.70	58.70	1.573	$0\bar{2}4$	4	3
28.34	28.34	3.150	$\bar{2}20$	39	30	58.80		1.570	$0\bar{8}1$	3	
30.14	30.14	2.965	$1\bar{3}1$	25	20	59.23	59.23	1.560	351	3	3
30.23		2.956	$\bar{2}\bar{2}2$	16		60.41	60.46	1.532	$\bar{4}24$	2	2
30.49	30.52	2.931	$0\bar{2}2$	12	19	61.50	61.48	1.508	$\bar{2}\bar{8}1$	4	3
30.53		2.928	$0\bar{4}1$	18		61.77	61.78	1.502	$\bar{5}\bar{3}3$	5	3
31.25	31.25	2.862	131	15	9	63.53	63.52	1.464	280	7	5
31.50	31.50	2.840	$\bar{1}\bar{3}2$	4	3	63.83	63.94	1.458	063	6	4
34.00	34.00	2.637	$\bar{1}32$	11	7	63.95		1.456	$\bar{2}80$	5	
35.03	35.03	2.562	$\bar{2}\bar{4}1$	21	12	64.93	64.94	1.436	$\bar{4}61$	6	3
35.38	35.38	2.537	$\bar{3}\bar{1}2$	3	2	65.20	65.20	1.431	262	6	4
35.98	35.98	2.496	$2\bar{2}1$	3	2	65.40		1.427	$\bar{4}62$	5	
36.81	36.82	2.442	$\bar{2}41$	15	9	65.48	65.42	1.425	$2\bar{4}3$	4	4
36.98	36.96	2.431	$\bar{1}\bar{5}1$	6	5	65.60		1.423	$\bar{5}14$	2	
37.35	37.36	2.408	240	5	4	66.07	66.06	1.414	114	4	2
37.46		2.401	$\bar{1}50$	3		67.13	67.16	1.394	$\bar{5}\bar{3}4$	4	3
37.66		2.388	$\bar{2}40$	3		67.44	67.46	1.389	$\bar{1}90$	2	2
37.68	37.68	2.387	310	2	3	67.49		1.388	460	3	
37.80		2.380	$\bar{3}10$	3		67.90	67.90	1.380	$1\bar{3}4$	4	3
38.83	38.83	2.319	$\bar{3}\bar{3}1$	12	7	68,06	68.04	1.377	243	3	3
39.59	39.59	2.276	$\bar{1}13$	3	2	68.57	68.37	1.372	$\bar{4}05$	4	2
40.17	40.18	2.244	$\bar{3}31$	3	2	68.92	68.92	1.362	$\bar{4}\bar{2}5$	4	2
41.27	41.30	2.187	042	3	5	69.51		1.352	$\bar{1}\bar{9}2$	5	
41.51		2.186	$1\bar{5}1$	5		69.55	69.54	1.352	$\bar{6}02$	6	6
42.53	42.53	2.125	060	12	7	69.74		1.348	$\bar{1}15$	4	
42.73	42.73	2.116	151	5	5	70.00	69.98	1.344	402	7	3
43.32	43.32	2.088	$\bar{3}13$	2	2	70.73	70.73	1.332	$\bar{6}\bar{2}2$	2	2
43.58	43.58	2.077	$2\bar{4}1$	8	4	70.97	70.97	1.328	$\bar{1}\bar{3}5$	4	3
44.54	44.54	2.034	241	3	1	74.00	74.00	1.281	$\bar{4}\bar{8}2$	5	3
45.33	45.34	2.001	$\bar{4}01$	3	2	74.85	74.84	1.268	$2\bar{8}2$	5	4
45.85	45.84	1.979	061	4	3	75.76	75.74	1.256	$\bar{5}\bar{3}5$	3	2
47.16	47.16	1.927	$2\bar{2}2$	4	2	77.98	77.98	1.225	282	5	3
48.05	48.06	1.893	$\bar{4}22$	12	7	78.31	78.30	1.221	$\bar{4}82$	4	2
48.16	48.16	1.889	$\bar{3}\bar{5}1$	3	8	78.91	78.91	1.213	600	4	2
48.19		1.888	222	9		81.93	81.96	1.176	$\bar{3}16$	3	2
49.28	49.28	1.849	$\bar{4}03$	13	7	82.93	82.93	1.164	353	2	2
49.49	49.49	1.842	260	4	4	85.39	85.40	1.137	640	2	1
49.83	49.98	1.830	$1\bar{1}3$	2	9	85.43		1.136	$\bar{1}\bar{9}4$	2	
49.86		1.829	$\bar{2}60$	8		85.97	85.90	1.131	$\bar{6}40$	2	1

TABLE 3. CALCULATED POWDER DATA FOR HIGH ALBITE (An_0)

2θ (INT)	2θ (P)	d	hkℓ	I_{INT}	I_P
13.74	13.76	6.445	$\bar{1}10$	9	16
13.78		6.425	020	10	
13.93	13.93	6.356	001	4	
15.22	15.22	5.822	$\bar{1}\bar{1}1$	6	6
15.69	15.70	5.648	$\bar{1}11$	6	5
22.04	22.04	4.032	$\bar{2}01$	100	84
22.90	22.90	3.884	$1\bar{1}1$	23	20
23.71	23.72	3.752	$\bar{1}30$	45	61
23.73		3.750	111	30	
24.46	24.46	3.639	130	30	28
24.56		3.625	$\bar{1}\bar{3}1$	9	
25.66	25.66	3.472	$\bar{1}\bar{1}2$	9	8
26.08	26.04	3.422	$\bar{2}\bar{2}1$	2	3
26.46	26.46	3.368	$\bar{1}12$	18	15
27.68	27.84	3.223	$\bar{2}20$	43	100
27.77		3.212	040	68	
27.86		3.203	$\bar{2}02$	83	
28.08	28.08	3.178	002	100	88
28.54	28.54	3.127	220	35	30
29.62	29.62	3.016	$1\bar{3}1$	18	14
30.31	30.31	2.949	$0\bar{4}1$	22	19
30.52	30.52	2.929	$0\bar{2}2$	16	15
30.71	30.70	2.911	$\bar{2}\bar{2}2$	10	10
31.56	31.56	2.835	131	21	17
31.79	31.79	2.815	$\bar{1}\bar{3}2$	6	6
33.73	33.73	2.656	$\bar{1}32$	10	7
35.45	35.66	2.532	$2\bar{2}1$	2	23
35.65		2.518	$\bar{2}\bar{4}1$	24	
35.68		2.516	$\bar{3}\bar{1}2$	3	
35.69		2.515	$1\bar{1}2$	3	
35.82	35.80	2.507	$\bar{2}41$	16	
36.61	36.61	2.455	$\bar{2}40$	3	4
36.91	36.91	2.435	221	3	3
37.20	37.20	2.417	$\bar{1}\bar{5}1$	3	3
37.37	37.37	2.407	$\bar{3}10$	3	3
37.86	37.94	2.376	310	3	6
37.95		2.371	240	7	
38.22	38.22	2.354	$\bar{1}51$	2	2
39.16	39.16	2.300	$\bar{3}31$	5	4
39.52	39.52	2.280	$\bar{3}\bar{3}1$	7	6
39.75	39.75	2.268	$\bar{1}13$	4	3
42.19	42.19	2.142	060	11	8
42.63	42.63	2.121	$2\bar{4}1$	12	10
43.01	43.01	2.103	151	5	4
43.21	43.20	2.093	$\bar{3}13$	3	3
44.96	44.96	2.016	$\bar{4}02$	3	3
45.18	45.18	2.007	$\bar{4}01$	3	3
45.61	45.61	1.989	061	5	5
46.78	46.80	1.942	$2\bar{2}2$	4	3
47.19	47.32	1.926•	$\bar{4}\bar{2}2$	3	7
47.32		1.921	$\bar{4}22$	9	
48.52	48.54	1.876	$\bar{2}60$	6	8
48.56		1.875	222	7	
49.35	49.35	1.847	$\bar{4}03$	11	8
49.69	49.70	1.835	$0\bar{6}2$	4	4
49.89	49.96	1.828	$1\bar{1}3$	3	11
49.92		1.827	$0\bar{4}3$	3	
49.97		1.825	400	11	

2θ (INT)	2θ (P)	d	hkl	I_{INT}	I_P
50.13	49.96	1.820	260	5	11
50.86	50.'90	1.795	$\bar{1}70$	3	7
50.91		1.794	113	8	
51.53	51.53	1.773	$\bar{2}04$	21	14
52.42	52.42	1.745	$2\bar{4}2$	5	5
52.60	52.60	1.740	420	3	3
52.73	52.70	1.736	$\bar{2}\bar{2}4$	3	3
53.18	53.18	1.722	062	3	3
53.42	53.54	1.715	$\bar{4}41$	3	5
53.55		1.711	$\bar{4}\bar{4}2$	6	
53.79	53.76	1.704	$\bar{4}42$	3	3
55.67	55.67	1.651	242	4	3
57.12	57.12	1.612	353	4	3
58.92	58.90	1.568	$0\bar{2}4$	2	3
60.10	60.10	1.540	351	3	3
61.17	61.17	1.515	$\bar{2}44$	2	2
62.10	62.10	1.495	$\bar{2}\bar{8}1$	5	4
62.33	62.33	1.490	$\bar{2}80$	6	5
62.69	62.69	1.482	$\bar{5}\bar{3}3$	4	4
62.93	62.93	1.477	$\bar{4}61$	5	6
63.28	63.26	1.470	$\bar{5}33$	2	3
63.52	63.52	1.465	$\bar{4}62$	2	3
63.87	63.87	1.457	063	5	4
64.15	64.15	1.452	280	5	3
64.84	64.84	1.438	$2\bar{4}3$	4	3
65.41	65.41	1.427	$\bar{5}14$	3	2
65.89	65.90	1.418	262	3	3
66.43	66.43	1.407	$\bar{2}\bar{6}4$	2	3
66.43		1.407	114	2	
67.25	67.28	1.392	190	3	3
67.32		1.391	441	2	
67.78	67.80	1.382	$\bar{1}91$	2	5
67.80		1.382	$\bar{4}63$	3	
67.82		1.382	$1\bar{3}4$	5	
68.12	68.12	1.376	$\bar{5}\bar{3}4$	3	3
68.69	68.72	1.366	243	2	5
68.72		1.366	460	2	
68.73		1.366	$\bar{4}05$	4	
69.35	69.38	1.355	$\bar{6}02$	6	5
69.50		1.352	$\bar{1}\bar{9}2$	5	
69.72	69.90	1.349	$\bar{4}\bar{2}5$	2	6
69.91		1.346	402	7	
70.15		1.342	$\bar{1}15$	3	
71.45	71.44	1.320	$\bar{1}\bar{3}5$	3	3
73.30	73.30	1.291	$2\bar{8}2$	3	3
75.50	75.52	1.259	$\bar{4}\bar{8}2$	5	4
75.91	75.92	1.253	$\bar{4}82$	3	3
75.94		1.253	$\bar{6}42$	2	
76.85	76.84	1.240	$\bar{5}\bar{3}5$	2	2
76.89		1.240	083	1	
78.56	78.68	1.217	442	1	4
78.62		1.217	600	4	
78.73		1.215	282	4	
82.35	82.40	1.171	$\bar{3}16$	2	2
82.41		1.170	$0\bar{8}4$	2	
83.87	83.88	1.154	353	2	2
84.07		1.151	$\bar{6}40$	2	

TABLE 4. CALCULATED POWDER DATA FOR OLIGOCLASE (An_{29})

2θ(INT)	2θ(P)	d	hkℓ	I_{INT}	I_P	2θ(INT)	2θ(P)	d	hkℓ	I_{INT}	I_P
13.81	13.82	6.412	$\bar{1}10$	6	5	49.87	49.86	1.829	260	5	11
15.13	15.13	5.856	$\bar{1}\bar{1}1$	4	2	49.94		1.826	$0\bar{4}3$	3	
18.98	18.98	4.675	$0\bar{2}1$	3	2	50.12		1.820	$\bar{2}62$	3	
21.99	21.99	4.042	$\bar{2}01$	93	52	50.78	50.78	1.798	113	10	5
22.93	22.93	3.879	$1\bar{1}1$	17	10	51.41	51.41	1.777	$\bar{2}04$	24	10
23.64	23.64	3.763	111	31	19	52.55	52.58	1.741	$\bar{2}\bar{2}4$	4	4
23.89	23.89	3.725	$\bar{1}30$	41	24	52.63		1.739	$2\bar{4}2$	5	
24.34	24.34	3.657	130	29	18	53.11	53.14	1.724	$\bar{4}\bar{4}2$	8	5
24.45		3.640	$\bar{1}\bar{3}1$	12		53.17		1.723	062	3	
25.58	25.58	3.483	$\bar{1}\bar{1}2$	13	8	53.75	53.78	1.705	$\bar{4}41$	3	2
25.83	25.83	3.449	$\bar{2}\bar{2}1$	5	3	53.86	53.86	1.702	$\bar{4}\bar{4}1$	2	2
26.44	26.44	3.371	$\bar{1}12$	22	12	54.09	54.09	1.695	$\bar{4}42$	4	2
27.78	27.82	3.211	$\bar{2}02$	87	100	54.44	54.44	1.685	$\bar{2}24$	4	3
27.83		3.206	$\bar{2}20$	46		55.40	55.40	1.658	242	3	1
27.83		3.206	040	67		57.38	57.38	1.606	$\bar{3}53$	5	3
28.03	28.03	3.184	002	100	64	58.50	58.56	1.578	$\bar{5}11$	2	2
28.34	28.34	3.149	220	40	25	58.59		1.575	$\bar{4}\bar{2}4$	3	
29.77	29.77	3.001	$1\bar{3}1$	23	12	58.84	58.84	1.569	$0\bar{2}4$	3	2
30.38	30.38	2.942	$0\bar{4}1$	23	15	59.71	59.71	1.549	351	3	1
30.51	30.52	2.929	$0\bar{2}2$	16	18	60.08	60.10	1.540	$\bar{4}24$	2	1
30.53		2.928	$\bar{2}\bar{2}2$	14		61.87	61.86	1.500	$\bar{2}\bar{8}1$	5	3
31.42	31.42	2.847	131	20	10	62.24	62.24	1.492	$\bar{5}\bar{3}3$	5	3
31.70	31.70	2.823	$\bar{1}\bar{3}2$	5	4	62.81	62.81	1.480	$\bar{2}80$	6	3
33.80	33.80	2.651	$\bar{1}32$	13	7	63.44	63.44	1.466	$\bar{4}61$	6	4
35.41	35.42	2.535	$\bar{2}\bar{4}1$	26	14	63.44		1.466	$\bar{5}33$	3	
35.50		2.529	$\bar{3}\bar{1}2$	5		63.81	63.88	1.459	063	5	4
35.56		2.524	$2\bar{2}1$	3		63.90		1.457	280	5	
35.68		2.516	$1\bar{1}2$	3		63.99		1.455	$\bar{4}62$	5	
36.08	36.08	2.489	$\bar{2}41$	17	9	64.99	64.99	1.435	$2\bar{4}3$	3	2
36.72	36.74	2.447	221	3	2	65.32	65.32	1.429	$\bar{5}14$	4	2
36.89	36.90	2.436	$\bar{2}40$	3	3	65.58	65.56	1.423	262	4	2
37.12	37.12	2.422	$\bar{1}\bar{5}1$	4	3	66.27	66.26	1.410	114	2	2
37.39	37.39	2.405	$\bar{3}10$	3	2	67.20	67.20	1.393	190	3	2
37.69	37.70	2.386	310	3	4	67.67	67.70	1.384	$\bar{5}\bar{3}4$	5	3
37.70		2.386	240	6		67.82	67.80	1.382	$1\bar{3}4$	5	3
39.21	39.21	2.298	$\bar{3}\bar{3}1$	8	4	68.40	68.52	1.371	243	3	3
39.39	39.38	2.288	$\bar{3}31$	6	3	68.54		1.369	$\bar{4}05$	5	
39.68	39.68	2.271	$\bar{1}13$	3	2	69.16	69.16	1.358	$\bar{6}02$	8	4
40.77	40.76	2.213	$1\bar{5}1$	3	2	69.39	69.48	1.354	$\bar{4}\bar{2}5$	4	4
41.82	41.82	2.160	$\bar{2}23$	3	2	69.50		1.352	$\bar{1}\bar{9}2$	6	
42.29	42.29	2.137	060	10	5	69.77	69.78	1.348	402	7	3
42.88	42.88	2.109	151	7	8	70.00		1.344	$\bar{1}15$	4	
42.89		2.109	$2\bar{4}1$	12		71.02	71.04	1.327	$\bar{5}53$	3	2
43.18	43.16	2.095	$\bar{3}13$	4	3	71.30	71.30	1.323	$\bar{1}\bar{3}5$	4	3
44.84	44.86	2.021	$\bar{4}02$	3	3	73.76	73.76	1.285	$2\bar{8}2$	4	2
45.08	45.08	2.011	$\bar{4}01$	3	2	74.92	74.92	1.267	$\bar{4}\bar{8}2$	5	3
45.66	45.66	1.987	061	4	3	76.11	76.14	1.251	$\bar{6}\bar{4}3$	3	2
46.85	46.86	1.939	$2\bar{2}2$	3	3	76.27	76.26	1.248	$\bar{6}42$	3	2
47.41	47.41	1.917	$\bar{4}22$	13	6	76.55	76.55	1.245	$\bar{4}82$	4	2
48.37	48.37	1.882	222	8	4	78.39	78.42	1.220	282	4	3
48.91	48.91	1.862	$\bar{2}60$	6	4	78.44		1.219	600	3	
49.21	49.21	1.852	$\bar{4}03$	11	5	79.22	79.18	1.209	$\bar{3}55$	3	2
49.79	49.86	1.831	$0\bar{6}2$	5	11	82.17	82.17	1.173	$\bar{3}16$	3	1
49.86		1.829	400	13		84.40	84.44	1.148	$\bar{6}40$	3	1
						84.62	84.58	1.145	$\bar{2}65$	2	1

TABLE 5. CALCULATED POWDER DATA FOR BYTOWNITE (An_{80})

2θ(INT)	2θ(P)	d	hkℓ	I_{INT}	I_P
12.94	12.94	6.839	$\bar{1}\bar{1}1$	2	2
13.63	13.63	6.498	$\bar{1}10$	9	9
13.80	13.80	6.417	020	9	9
13.92		6.364	002	4	
15.25	15.25	5.809	$\bar{1}\bar{1}2$	10	8
15.71	15.71	5.640	$\bar{1}12$	5	5
17.65	17.65	5.026	$\bar{1}\bar{2}1$	2	2
18.90	18.90	4.694	$0\bar{2}2$	2	1
20.36	20.36	4.361	022	2	2
22.00	22.00	4.041	$\bar{2}02$	100	82
22.73	22.73	3.913	$1\bar{1}2$	31	26
23.61	23.64	3.767	$\bar{1}30$	29	48
23.66		3.761	112	37	
24.22	24.22	3.675	200	3	4
24.51	24.51	3.631	130	23	20
24.61		3.618	$\bar{1}\bar{3}2$	5	
25.69	25.69	3.468	$\bar{1}\bar{1}4$	3	3
26.52	26.52	3.360	$\bar{1}14$	8	7
27.45	27.45	3.249	$\bar{2}20$	29	27
27.80	27.82	3.209	040	84	93
27.91	27.91	3.197	$\bar{2}04$	86	100
28.04	28.04	3.181	004	86	85
28.49	28.49	3.132	220	23	21
29.42	29.42	3.036	$1\bar{3}2$	12	10
30.26	30.26	2.954	$0\bar{4}2$	17	15
30.43	30.43	2.938	$0\bar{2}4$	16	14
30.78	30.78	2.905	$\bar{2}\bar{2}4$	9	7
31.59	31.59	2.832	132	7	5
31.81	31.81	2.813	$\bar{1}\bar{3}4$	4	4
32.10	32.12	2.788	221	1	2
33.06	33.06	2.709	202	2	1
33.84	33.84	2.649	$\bar{1}34$	4	3
35.14	35.14	2.554	$2\bar{2}2$	3	3
35.73	35.73	2.513	$\bar{2}\bar{4}2$	2	19
35.73		2.513	$\bar{2}42$	7	
35.91	35.88	2.501	$\bar{3}14$	9	10
36.38	36.38	2.469	$\bar{2}40$	8	10
36.53		2.459	114	13	
36.59	36.56	2.456	$\bar{1}50$	12	17
36.80		2.442	222	2	
37.26	37.26	2.413	$\bar{1}\bar{5}2$	5	4
37.60	37.60	2.392	150	9	7
38.00	38.00	2.368	240	13	9
38.35	38.35	2.347	$0\bar{4}4$	2	3
38.69	38.69	2.327	$\bar{3}\bar{1}5$	1	2
38.95	39.00	2.312	$\bar{3}\bar{6}2$	3	5
39.03		2.308	$\bar{2}\bar{4}4$	4	
39.53	39.53	2.280	$\bar{3}\bar{3}2$	12	9
39.81	39.81	2.264	$\bar{1}16$	10	8
40.43	40.43	2.230	$\bar{2}\bar{2}6$	2	2
40.56	40.54	2.224	$\bar{2}44$	2	2
41.40	41.40	2.181	$\bar{3}34$	3	3
41.92	41.94	2.155	$\bar{2}26$	2	3
42.25	42.28	2.139	060	6	19
42.29		2.137	$2\bar{4}2$	24	
42.68	42.66	2.118	134	2	3
42.96	42.98	2.105	$\bar{1}\bar{3}6$	4	4
43.12	43.12	2.098	152	5	5
43.29	43.28	2.090	$\bar{3}16$	4	4
44.86		2.020	$\bar{4}04$	3	
44.87	44.88	2.020	$\bar{1}54$	7	8
44.95		2.017	$\bar{4}02$	5	
45.26	45.24	2.004	$3\bar{1}2$	3	3
45.73	45.73	1.984	062	2	2
46.11	46.10	1.968	312	2	3
46.41	46.41	1.956	$2\bar{2}4$	2	2
46.91	46.91	1.937	$\bar{2}\bar{4}6$	4	4
47.16	47.16	1.927	$\bar{4}\bar{2}4$	2	8
47.16		1.927	$\bar{4}24$	10	
48.36	48.38	1.882	$\bar{3}52$	2	7
48.41		1.880	224	6	
49.17	49.37	1.853	$\bar{3}\bar{5}2$	2	8
49.37		1.846	$\bar{4}06$	11	
49.57		1.839	$0\bar{6}4$	2	
49.61	49.60	1.838	400	11	10
49.66		1.836	$1\bar{1}6$	2	
50.25	50.25	1.816	260	6	4
50.45	50.43	1.809	$\bar{2}\bar{6}4$	2	3
50.78	50.78	1.798	116	8	8
50.81		1.797	$\bar{1}70$	4	
51.12	51.16	1.787	$\bar{4}20$	2	3
51.33	51.33	1.780	$\bar{1}\bar{7}2$	2	3
51.64	51.64	1.770	$\bar{2}08$	18	11
52.00	52.00	1.759	$2\bar{4}4$	8	6
52.33		1.748	$\bar{2}64$	1	
52.37	52.38	1.747	420	2	4
52.42		1.745	$\bar{1}72$	1	
52.80	52.80	1.734	$\bar{2}\bar{2}8$	3	4
52.81		1.734	$1\bar{3}6$	2	
53.33	53.33	1.718	064	3	3
53.60	53.60	1.710	$\bar{4}\bar{4}4$	7	9
53.61		1.710	$\bar{4}44$	6	
54.62	54.62	1.680	$\bar{2}28$	3	2
55.64	55.64	1.652	244	6	3
56.58	56.58	1.627	$\bar{3}\bar{3}8$	1	2
57.10	57.04	1.615	$\bar{4}\bar{4}6$	1	1
57.44	57.44	1.604	080	3	2
57.97	57.97	1.591	008	1	1
58.27	58.27	1.583	$0\bar{8}2$	2	2
58.76	58.76	1.571	$0\bar{2}8$	2	2
59.03	59.03	1.564	$\bar{4}\bar{2}8$	2	2
60.26	60.10	1.536	$\bar{2}66$	1	2
61.34	61.36	1.511	$\bar{2}48$	3	2
62.14		1.494	$\bar{2}80$	3	
62.26	62.26	1.491	$\bar{2}\bar{8}2$	5	5
62.32		1.490	$\bar{1}\bar{7}6$	1	
62.56	62.56	1.485	$\bar{4}62$	4	3
62.72	62.72	1.481	$\bar{5}36$	3	3
62.94		1.477	084	1	
63.32	63.32	1.469	$\bar{4}64$	4	4
64.04	64.04	1.454	066	3	3
64.33	64.34	1.448	280	2	3
64.35		1.448	$2\bar{4}6$	3	

TABLE 6. CALCULATED POWDER DATA FOR ANORTHITE (An_{100})

2θ(INT)	2θ(P)	d	hkℓ	I_{INT}	I_P	2θ(INT)	2θ(P)	d	hkℓ	I_{INT}	I_P
13.01	13.01	6.807	$\bar{1}\bar{1}1$	9	8	45.22	45.20	2.005	$3\bar{1}2$	3	4
13.58	13.58	6.522	$\bar{1}10$	10	8	45.54	45.54	1.992	$\bar{1}36$	3	3
13.79	13.79	6.420	020	4	4	45.69	45.68	1.986	062	4	4
17.33	17.32	5.118	$1\bar{1}1$	3	2	46.16	46.14	1.966	312	3	4
17.73	17.73	5.002	$\bar{1}\bar{2}1$	2	1	46.38	46.38	1.958	$2\bar{2}4$	3	3
18.92	18.92	4.690	$0\bar{2}2$	17	14	47.04	47.04	1.932	$\bar{4}24$	11	9
20.95	20.95	4.240	003	2	2	47.32	47.32	1.921	$\bar{4}\bar{2}4$	5	4
22.01	22.01	4.039	$\bar{2}02$	58	48	48.10	48.10	1.892	$\bar{3}52$	2	4
22.71	22.71	3.916	$1\bar{1}2$	13	11	48.11		1.891	$\bar{2}60$	4	
23.52	23.52	3.783	$\bar{1}30$	30	28	48.47	48.47	1.878	224	9	7
23.62		3.767	$\bar{1}\bar{3}1$	5		49.27		1.849	$\bar{3}\bar{5}3$	2	
23.69	23.68	3.756	112	17	19	49.39	49.42	1.845	$\bar{2}46$	2	12
24.59	24.60	3.620	130	38	33	49.41		1.845	$\bar{4}06$	11	
24.71		3.603	$\bar{1}\bar{3}2$	13		49.61		1.838	$0\bar{6}4$	3	
25.37	25.37	3.510	$\bar{1}32$	4	4	49.62	49.62	1.837	400	18	16
25.63	25.76	3.476	$1\bar{3}1$	4	14	49.69		1.835	$1\bar{1}6$	4	
25.75		3.459	$\bar{1}\bar{1}4$	15		50.42	50.44	1.810	260	5	5
26.18	26.18	3.403	$\bar{2}\bar{2}2$	7	7	50.67	50.68	1.802	$\bar{2}\bar{6}4$	5	8
26.51	26.51	3.362	$\bar{1}14$	31	25	50.68		1.801	$\bar{1}70$	4	
27.35	27.35	3.261	$\bar{2}20$	64	52	50.81	50.81	1.797	116	10	9
27.79	27.79	3.210	040	53	63	51.69	51.69	1.768	$\bar{2}08$	26	17
27.93	27.93	3.194	$\bar{2}04$	100	100	51.91	51.88	1.761	$2\bar{4}4$	8	8
28.06	28.06	3.180	004	93	91	52.27	52.26	1.750	$\bar{1}72$	3	4
28.59	28.59	3.122	220	49	39	52.58	52.52	1.742	154	3	4
29.36	29.36	3.042	$1\bar{3}2$	23	18	52.67		1.738	$2\bar{6}2$	3	
30.27	30.27	2.952	$0\bar{4}2$	33	27	52.92	52.82	1.733	$\bar{4}42$	4	6
30.46	30.46	2.934	$0\bar{2}4$	20	19	52.93		1.730	$\bar{2}\bar{2}8$	3	
30.91	30.92	2.893	$\bar{2}\bar{2}4$	8	8	53.28		1.719	064	4	
31.64	31.64	2.828	132	27	20	53.35	53.34	1.717	$\bar{4}44$	4	7
31.92	31.92	2.804	$\bar{1}\bar{3}4$	11	9	53.48		1.713	046	3	
33.76	33.76	2.655	$\bar{1}34$	18	14	53.87	53.88	1.702	$\bar{4}\bar{4}4$	6	5
35.07	35.07	2.559	$2\bar{2}2$	5	6	54.59	54.58	1.681	$\bar{2}28$	5	4
35.50	35.54	2.529	$1\bar{1}4$	7	20	55.73	55.73	1.649	244	3	2
35.55		2.525	$\bar{2}42$	22		56.94	56.94	1.617	$\bar{3}56$	5	4
35.79	35.90	2.509	$\bar{3}\bar{1}4$	4	28	57.41	57.38	1.605	080	3	3
35.91		2.501	$\bar{2}\bar{4}2$	37		58.83	58.83	1.570	$0\bar{2}8$	3	3
36.88	36.88	2.437	222	5	6	59.35	59.32	1.557	$3\bar{3}4$	3	3
37.01		2.429	$\bar{3}10$	3		59.61	59.61	1.551	$\bar{3}\bar{1}9$	3	3
37.37	37.37	2.406	$\bar{1}\bar{5}2$	5	4	60.09		1.540	$\bar{4}28$	2	
37.73	37.72	2.384	310	3	4	60.22	60.26	1.537	$\bar{5}34$	2	4
38.13	38.14	2.360	$\bar{1}52$	3	5	60.27		1.536	352	4	
38.14		2.359	240	3		60.91		1.521	$2\bar{6}4$	2	
38.77	38.78	2.323	$\bar{3}32$	9	8	61.04	61.06	1.518	028	2	4
39.25	39.25	2.295	$\bar{1}\bar{5}3$	3	3	61.05		1.518	$\bar{1}\bar{1}9$	2	
39.71	39.72	2.270	$\bar{3}\bar{3}2$	6	7	61.08		1.517	$\bar{5}\bar{3}4$	2	
39.82		2.264	$\bar{1}16$	5		61.23		1.514	$\bar{2}48$	2	
40.28	40.28	2.239	$1\bar{5}2$	5	4	61.90	61.90	1.499	$\bar{2}80$	7	5
40.39		2.233	$\bar{2}44$	3		62.22	62.22	1.492	$\bar{4}62$	7	6
41.85	41.85	2.158	$\bar{2}26$	4	4	62.47	62.48	1.487	$\bar{2}\bar{8}2$	6	6
42.16	42.18	2.143	$2\bar{4}2$	19	17	62.49		1.486	334	2	
42.23		2.140	060	10		62.94		1.477	$\bar{5}36$	3	
42.69	42.69	2.118	$\bar{2}\bar{4}5$	3	4	62.97	62.96	1.476	$0\bar{8}4$	2	10
43.17	43.17	2.095	152	14	10	62.97		1.476	$\bar{4}64$	6	
43.79	43.79	2.067	$0\bar{4}5$	3	3	62.98		1.476	$\bar{5}\bar{3}6$	4	
44.75	44.75	2.025	$\bar{1}54$	3	3	62.99		1.476	$\bar{5}\bar{3}2$	1	
44.88	44.94	2.019	$\bar{4}04$	3	5	64.00	64.00	1.455	066	9	5
44.96		2.016	$\bar{4}02$	5		64.30	64.30	1.449	$2\bar{4}6$	4	3
						64.51	64.51	1.444	280	3	3

TABLE 7. "c" AND "d" REFLECTIONS IN ANORTHITE (An_{100})

2θ (INT)	d	hkl	I_{INT}	2θ (INT)	d	hkl	I_{INT}
6.95	12.718	001	0.6	29.17	3.061	041	1.1
13.01	6.807	$\bar{1}\bar{1}1$	9.0	30.60	2.921	$2\bar{2}1$	0.6
15.00	5.904	$0\bar{2}1$	1.2	30.96	2.889	140	0.6
15.10	5.869	$0\bar{1}2$	0.6	32.10	2.781	221	2.1
15.90	5.573	021	0.7	32.90	2.723	$\bar{2}05$	1.8
17.33	5.118	$1\bar{1}1$	2.6	33.79	2.653	$0\bar{4}3$	1.7
19.32	4.594	$\bar{1}22$	1.1	34.23	2.620	$\bar{1}33$	0.6
19.96	4.448	$\bar{1}\bar{1}3$	1.1	35.11	2.556	$\bar{3}\bar{1}1$	2.1
20.58	4.316	$\bar{1}13$	0.7	35.28	2.544	005	0.5
20.95	4.240	003	2.4	35.29	2.543	$\bar{2}\bar{2}5$	1.8
23.42	3.798	$\bar{1}31$	0.8	36.34	2.472	$\bar{2}25$	1.4
23.62	3.767	$\bar{1}\bar{3}1$	5.0	36.83	2.440	$\bar{1}\bar{5}1$	1.3
24.12	3.689	$\bar{2}03$	1.5	36.90	2.436	$\bar{2}\bar{4}3$	0.6
24.31	3.661	$0\bar{2}\bar{3}$	0.9	37.73	2.384	$1\bar{5}1$	1.1
25.63	3.476	$1\bar{3}1$	4.4	38.78	2.322	$\bar{3}\bar{1}5$	1.5
26.00	3.426	023	1.2	39.01	2.301	025	1.9
27.42	3.253	131	0.6	39.25	2.295	$\bar{1}\bar{5}3$	2.7
27.63	3.229	$\bar{1}\bar{3}3$	1.5	39.51	2.280	$\bar{3}31$	0.9
27.75	3.215	$\bar{2}\bar{2}3$	1.0	39.72	2.269	$\bar{3}\bar{3}3$	0.8
28.88	3.092	$1\bar{1}\bar{3}$	0.7				

Thus, profiles of observed peaks are convolutions of the X-ray spectral distribution and are strongly influenced by instrumental aberrations, sample alignment, and effects that relate to particle size, strain and homogeneity of the sample. Thus, the calculated peak intensities reflect assumptions that have been made concerning the shape of the diffraction maxima as well as overlap of adjacent maxima. They are: (1) the diffraction maxima from both $K\alpha_1$ and $K\alpha_2$ have Cauchy profiles; (2) the width of the profile at half maximum is dependent on the diffraction angle and can be estimated without evaluating the individual factors mentioned above which influence it: (3) adjacent maxima will overlap to produce a single I_P when separated by less than one half-width.

The relation of half-width to 2θ in (2) is based on empirical data from α-Al_2O_3 and Si. The data were measured on diffractometer traces of uncemented powders in standard holders, using a Norelco wide-angle goniometer over the whole 2θ range (1/4° 2θ.min scan using a pulse-height analyzer, 1° divergent and scattering slits and 0.003 in. receiving slits). The half-widths recorded on Al_2O_3 and Si are more narrow (0.10° at $2\theta=40°$) than recorded in plagioclase scanned under similar conditions (0.10–0.16° at $2\theta=40°$). This is due in large part to the greater compositional variation in samples of natural silicates. The I_P data of Tables 2–7 are based on the half-width versus 2θ function determined on Al_2O_3 and Si extrapolated to a half-width of 0.16° at 40° 2θ.

The intensities I_{INT} and I_P (Tables 2–7) are directly related to intensities obtained from diffractometry which utilizes flat samples and thus eliminates absorption corrections for materials with moderate absorption. Use of cylindrical samples in Debye-Scherrer cameras requires an absorption correction; and within the angular range reported, the resultant I_{INT} and I_P differ so slightly from those tabulated for flat samples (see Table 8) that they have not been included in Table 2–7. In general, absorption in cylindrical mounts causes the front reflection to be relatively weaker than the back reflection region, the effect bring pronounced in compounds containing the heavier elements.

TABLE 8. EXAMPLES OF INTEGRATED INTENSITIES IN ANORTHITE FOR CYLINDRICAL (*C*) AND FLAT SAMPLES (*F*)

hkl	2θ CuK$_\alpha$ (deg)	$I_{INT}(F)$	$I_{INT}(C)$
$\bar{1}\bar{1}1$	13.01	9.0	7.9
$\bar{2}02$	22.01	58.3	54.9
$\bar{2}04$	27.93	100.0	100.0
152	43.17	14.0	16.7
066	64.00	8.8	13.5

In the case of calculated integrated intensities (I_{INT}), the strongest peak was set to 100 (002 for albite and oligoclase; $\bar{2}02$ and $\bar{2}04$ for bytownite and anorthite, respectively). Peak intensities (I_P), graphically displayed in Figures 1–4 and also included in Tables 2–6, are scaled to the maximum observed which was set at 100.

In view of the relatively narrow spectra of spacings, normally measured and indexed in these complex powder patterns, an unresolved CuKα radiation was used in the computations. The total number of reflections that could be calculated was limited by the code to 1000, thus restricting the maximum 2θ angle to 87° for *C*-centered cells and to 65° for primitive and body-centered cells. However, in consideration of space limitations, only those *hkl* reflections whose calculated integrated

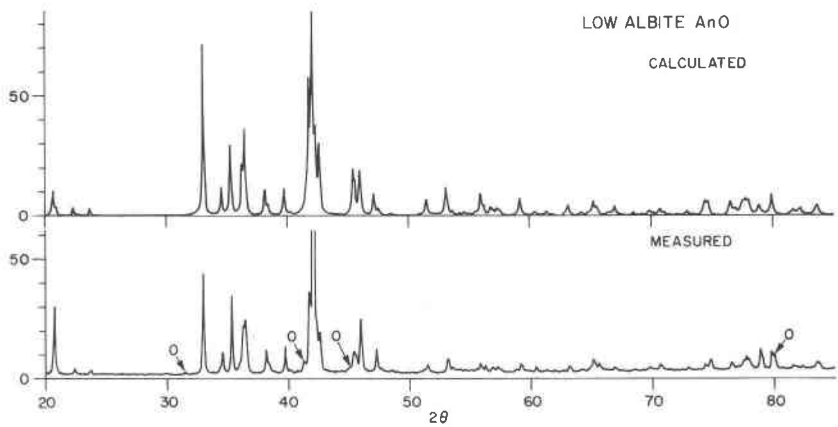

FIG. 1. Powder patterns at low albite, CrKα. (a) Calculated pattern of Ramona albite, (b) measured pattern of Amelia albite by William Parrish, Phillips Laboratories. Peaks marked "O" are due to impurities. (40 kVp/20mA, 10° take-off angle on point source, vacuum diffractometer, $\frac{1}{2}$°/min, time const = 2 sec, 2-$\frac{1}{2}$° angular aperature, 0.006 in. (0.05°) receiving slit, specimen rotated in its own plane.)

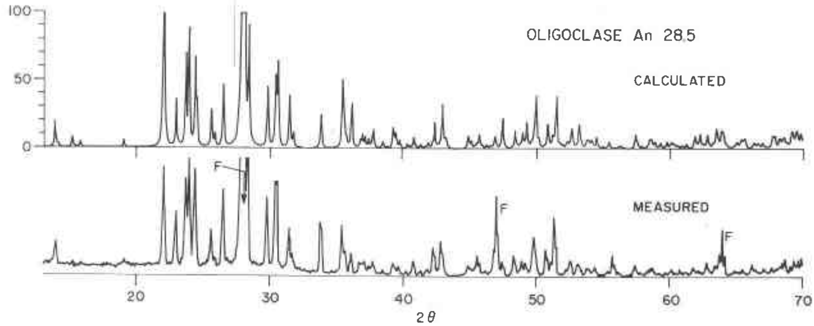

FIG. 2. Powder patterns of oligoclase, An_{29}, Mitchell Co., N.C., CuKα. (a) Calculated pattern, (b) measured pattern by D. B. Stewart, U.S.G.S. F = fluorite. (45kVp/20mA, 1° /min, time const = 4 sec, 1° divergent and anti-scatter slits, 0.006 in. receiving slit, pulse height analyzer.)

intensities met the following criteria were included in Tables 2–6:[1] $100I_{hkl}/I_{002} \geqq 2.4$ (albite and oligoclase); $100I_{hkl}/I_{\bar{2}02} \geqq 1.4$ (bytownite); and $100I_{hkl}/I_{\bar{2}04} \geqq 2.4$ for $2\theta = 0°–60°$ and $\geqq 1.4$ for $2\theta = 61°–65°$ (anorthite). In consideration of the importance of weak "c" reflections ($h+k$, even; l, odd) in distinguishing anorthite and transitional anorthite, a separate Table 7 lists "c" and "d" reflections ($h+k$, even; l odd and $h+k$,

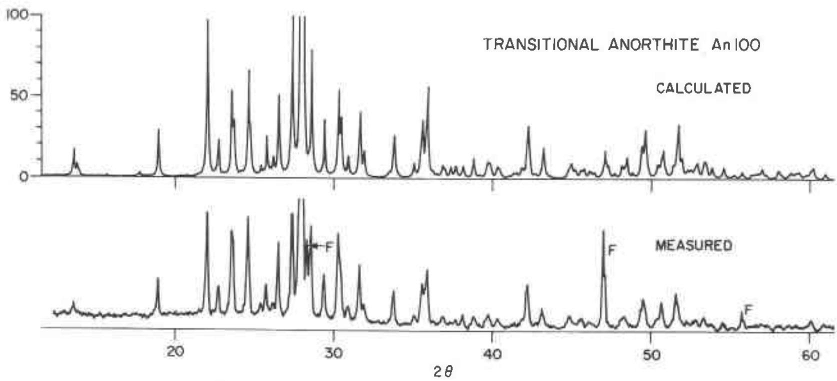

FIG. 3. Powder patterns of synthetic transitional anorthite, An_{100}, ANS-26 (Stewart, 1967, p. 50), CuKα. (a) Calculated pattern, (b) measured pattern by D. B. Stewart, U.S.G.S. F = fluorite. (Experimental conditions as in Fig. 2b.)

[1] 20 receive unabridged Tables 2–6, order NAPS Document-00038 from ASIS National Auxiliary Publications Service, c/o CCM Information Sciences, Inc., 22 West 34th Street, New York, N. Y. 10001; remitting \$2.00 for microfiche or \$6.00 for photocopies.

odd; l, even respectively) for anorthite. Most are too weak to be included in Table 6. Criterion for inclusion in Table 7 is $100I_{hkl}/I_{\bar{2}04}>0.05$ and $2\theta<40°$.

Results and Conclusions

Calculated diffractometer traces are juxtaposed with real diffractometer traces in Figures 1–4 to illustrate their generally good agreement. Except for Figure 1, real traces are measured on smear mounts; no effort was made to eliminate preferred orientation in any of the four.

The calculated traces in Figures 1–4 are based on an assumed half-width at 40° 2θ of 0.12–0.13° which is smaller than that used to calculate

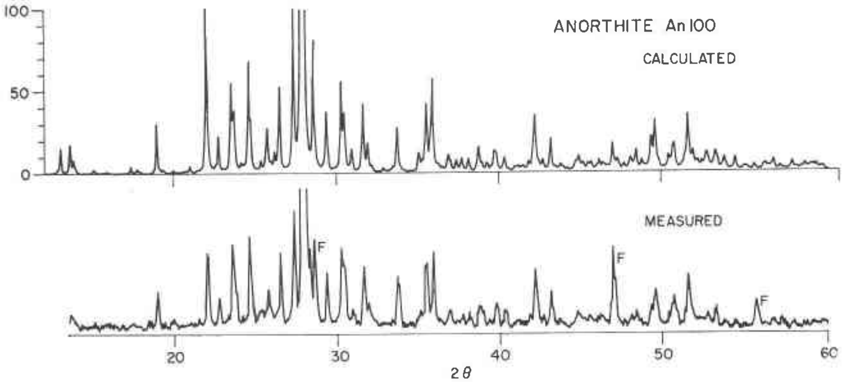

FIG. 4. Powder patterns of synthetic anorthite, An_{100}, ANS-305 (Stewart, 1967, p. 50), CuKα. (a) Calculated pattern, (b) measured pattern by D. B. Stewart. F = fluorite (experimental conditions as in Fig 2b).

the I_P of Tables 2–7 (0.16°). Use of the smaller value was necessary in order to match the good resolution in the real patterns. These are not only of high quality but also include traces from synthetic plagioclases. In contrast to the natural plagioclases, the latter are more uniform in composition and therefore also in unit cell size; as a consequence, line broadening from these sources is not expected. The 0.16° half-width used for calculated I_P in the Tables and Figure 5 is considered to be a better approximation for natural plagioclases. But even use of the large half-width results in plots with resolution that may not be found in natural patterns. For example, in the high albite trace (Fig. 5), resolution of $0\bar{4}1$, $0\bar{2}2$, and $\bar{2}22$ at $2\theta\sim30.5$ and 131 and $\bar{1}\bar{3}2$ at $2\theta\sim31.7°$ has no counterpart in the measured patterns recorded in Figure 1 (Smith and Yoder, 1956) and Figure 1 (Bambauer *et al.*, 1967). The lack of resolution may reflect incorrect overlap criterion used in the calculated

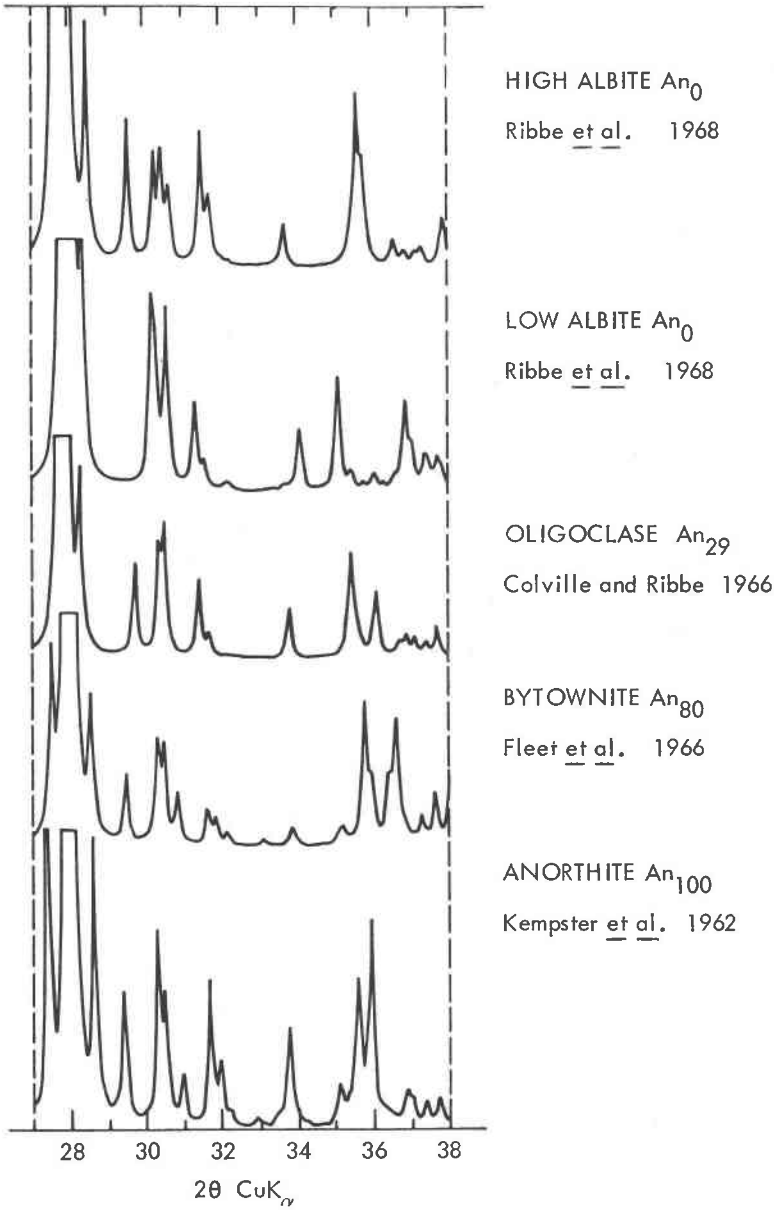

FIG. 5. Portions of calculated powder patterns.

model, which is determined by the half-width chosen, or slight differences in lattice parameters in the various plagioclases used.

The chief differences in the juxtaposed patterns is in the intensities of certain peaks. For example, in real traces of oligoclase, anorthite and transitional anorthite (Figs. 2–4), the $\bar{2}0l$ peaks at $2\theta \cong 22.0°$ are low relative to the calculated counterpart. The reasons for these differences are not certainly known, but are believed to be due to a preferred orientation of the particles on the slide mounts because of perfect (001) and (010) cleavages. Under these circumstances, lower intensities of $h00$, $h0l$ and hkl peaks would be anticipated as well as enhancement of $00l$, $0k0$ and $0kl$. In our experience, peak heights in synthetic materials, more closely resemble the calculated than do those in natural minerals. The observation is in keeping with an initial finer grain size in synthetics, which eliminates the need for further grinding and therefore the production of particles bounded by cleavages.

It is hoped that the calculated integrated and peak intensities presented here will serve as guides to indexing the complex patterns of the plagioclases. If so, the data will have helped to eliminate one important source of error in the process of reducing powder data to meaningful parameters, *vis.*, mis-identification of diffraction maxima.

For indexing complex patterns, we recommend use of the calculated I_{INT} and I_P of Tables 2–7 to recognize overlap, and in such cases to assess the likely contribution of each reflection to the observed peak maximum. As is well-known, overlap of a strong and a weak reflection can result in a single peak whose intensity is enhanced as well as skewed off the 2θ value associated with the stronger of the two. In the case where the ratio of the intensities is large, *e.g.* 10:1, the peak can be confidently associated with the hkl of the stronger, but if the ratio approaches 1:1 and the reflections do not exactly coincide, the d of the peak does not correspond to either reflection. Even in the case of closely spaced, but resolved reflections, the position of each is effected to some extent by proximity of the other. These considerations put a limit on the ultimate accuracy of lattice parameters calculated by least-square refinements of triclinic powder data assuming otherwise ideal conditions.

In resumé, I_P in calculated as well as measured powder patterns must be interpreted with discretion. These intensities are influenced by overlap of maxima and by line-broadening related to minor variations in sample, composition, particle size, instrumental abberations, strain, and sample alignment. In addition, preferred orientation, because of perfect cleavages and dimensional alignment of particles, is a factor that influences I_P. Nonetheless, the data presented here make reasonable allowance for many of these variables, and by doing so simulate natural patterns.

Acknowledgments

We are grateful to Paul Ribbe, A. Colville, Helen Megaw, and W. H. Taylor for making the results of their structure analyses available before publication. Comment and recommendations by D. B. Stewart and Helen Megaw have greatly improved the lucidity of the text. Finally, we are in debt to D. B. Stewart and W. Parrish for their high-quality diffractometry data on natural plagioclases which were used in the illustrations.

Work performed under the auspices of the U. S. Atomic Energy Commission.

References

Bambauer, H. U., M. Corlett, E. Eberhard and K. Viswanathan (1967) Diagrams for the determination of plagioclase using X-ray powder methods. Part III. *Schweiz. Mineral. Petrog. Mitt.*, **47**, 333–349.

Cole, W. F., H. Sorum and W. H. Taylor (1951) The structures of plagioclase feldspars. I. *Acta Crystallogr.*, **4**, 20–29.

Colville, A. A., and P. H. Ribbe (1966) The crystal structure of oligoclase. (abstr.) *Geol. Soc. Amer. Spec. Pap.*, **101**, 41.

Ferguson, R. B., R. V. Traill and W. H. Taylor (1958) The crystal structures of low-temperature and high-temperature albites. *Acta Crystallogr.*, **11**, 331–348.

Fleet, S. G., S. Chandrasekhar, and Helen D. Megaw (1966) The structure of bytownite ('body-centered anorthite'). *Acta Crystallogr.*, **21**, 782–801.

Kempster, C. J. E., Helen D. Megaw, and E. W. Radoslovich (1962) The structure of anorthite, $CaAl_2Si_2O_8$. I. Structure analysis. *Acta Crystallogr.*, **15**, 1005–1017).

Megaw, Helen D., C. J. E. Kempster, and E. W. Radoslovich (1962) The structure of anorthite, $CaAl_2Si_2O_8$. II. Description and discussion. *Acta Crystallogr.*, **15**, 1017–1035.

Ribbe, P. H., and Helen D. Megaw (1963) The structure of transitional anorthite. A comparison with primitive anorthite. *Norsk Geol. Tids.*, **42**, 158–167.

———, ———, and W. H. Taylor (1968) The albite structure. *Acta Crystallogr.* (in press).

Smith, D. K. (1968) Computer simulation of X-ray diffractometer traces. *Norelco Rep.*, **15**, 57–65.

——— (1967) A revised program for calculating X-ray powder diffraction patterns. Lawrence Rad. Lab. [*U. S. Clearinghouse Fed. Sci. Tech. Inform.*]**UCRL-50264.**

Smith, J. R., and H. S. Yoder (1956) Variations in X-ray powder diffraction patterns of plagioclase feldspars. *Amer. Mineral.*, **41**, 632–647.

Stewart, D. B. (1967) Four-phase curve in the system $CaAl_2Si_2O_8$-SiO_2-H_2O between 1 and 10 kb. *Schweiz. Mineral. Petrog. Mitt.*, **47**, 35–59.

Manuscript received, December 6, 1967; accepted for publication, March 17, 1968.